The Mt. Lewis Fault Zone: Tectonic Implications for Eastern San Francisco Bay

by
Janet T. Watt[1], David A. Ponce[2], Robert W. Simpson[3], Russell W. Graymer[4], Robert C. Jachens[5], and Carl M. Wentworth[6]

ABSTRACT

The Mount Lewis fault zone is a 25-km long system of faults that intersects the Calaveras Fault near a prominent segment boundary, suggesting a relationship between the two faults that has implications for eastern San Francisco Bay tectonics. Kilb and Rubin (2002) identified a main north-south-striking, right-lateral strike-slip fault plane and a number of small, steeply dipping, east-west faults from analysis of the 1986 $_{Mw}$ 5.7 Mt. Lewis earthquake and aftershocks and inferred the growth of a young fault. On the basis of two-dimensional (2D) and three-dimensional (3D) analysis of double-difference relocated seismicity, we confirm the presence of a main north-south Mt. Lewis fault zone and extend it to the Calaveras Fault. We identify two additional faults that appear to connect with the main north-south-striking fault zone and project upward to mapped surface structures: an unnamed fault located about 2-km east of the Mt. Lewis mainshock and a locally north-trending major lithostratigraphic fault boundary within the Franciscan Complex that is characterized by a distinct assemblage of serpentinite and high-grade schist. The major lithostratigraphic fault boundary joins the Mt. Lewis fault zone beneath the northern end of a serpentinite body. Magnetic modeling shows that a sliver of serpentinite extends to at least 2-3-km depth, with alignments of deeper seismicity extending up to the serpentinite. Although there is no dextral offset in mapped surface geology or observed surface rupture along the seismicity trend, there is a diffuse north-south topographic lineament that crosscuts the surrounding landscape and intersects the Calaveras Fault. The 25-km long Mt. Lewis fault zone extends southward from the Mt. Lewis earthquake epicenter and appears to intersect the Calaveras Fault near the epicenter of the 1984 M_w 6.2 Morgan Hill earthquake and the northern boundary of the Morgan Hill segment, suggesting that segmentation on the Calaveras Fault is related to deformation along the Mt. Lewis fault zone. In turn, motion on the Mt. Lewis fault zone may be influencing the surface morphology of the Calaveras Fault within the Morgan Hill segment. The Mt. Lewis seismicity trend is the largest in a series of N-S seismicity trends with right-lateral focal mechanisms located northeast of the Calaveras Fault that may be accommodating strain between the Calaveras and Greenville Faults.

INTRODUCTION

Recent advances in earthquake relocation using waveform cross correlation have allowed the 3D identification and mapping of discrete fault planes at depth based on detailed alignments of earthquake hypocenters (e.g. Waldhauser and Ellsworth, 2002; Kilb and Rubin, 2002; Schaff et al., 2002; Hardebeck et al., 2007). We use the seismicity catalog of Waldhauser and Schaff (2008) to identify and map fault surfaces in 3D associated with the Mt. Lewis seismicity trend (hereafter referred to as the Mt. Lewis trend). We then explore the relation of this structure to the Calaveras Fault and, more broadly, how it fits into the tectonic framework of the eastern San Francisco Bay area. This study is part of a larger effort to develop a 3D geologic framework model for the Hayward-Calaveras Fault System to investigate relationships between fault zone geology and fault behavior.

The Mt. Lewis trend represents a 25-km long zone of mainly micro-seismisity (< M_w 2) within the Diablo Range that encompasses the 1986 M_w 5.7 Mt. Lewis earthquake and aftershock sequence and extends southward to, but does not cross, the Calaveras Fault near the epicenter of the 1984 M_w 6.2 Morgan Hill earthquake (Figure 1). Studies of the aftershock distribution and focal mechanisms of the Mt. Lewis earthquake (Oppenheimer et al., 1992; Zhou, 1992) revealed a vertical north-south-striking, right-lateral stike-slip fault. Kilb and Rubin (2002) used seismic waveform cross correlation to achieve more precise relative locations for the Mt. Lewis earthquake and aftershocks and discovered numerous short (<1-km long) vertical east-west-trending left-lateral faults east of the main north-south stike-slip fault and north of the mainshock

[1] U.S. Geological Survey, 345 Middlesfield Rd., Menlo Park, CA 94025, jwatt@usgs.gov
[2] U.S. Geological Survey, 345 Middlesfield Rd., Menlo Park, CA 94025, ponce@usgs.gov
[3] U.S. Geological Survey, 345 Middlesfield Rd., Menlo Park, CA 94025, simpson@usgs.gov
[4] U.S. Geological Survey, 345 Middlesfield Rd., Menlo Park, CA 94025, rgraymer@usgs.gov
[5] U.S. Geological Survey, 345 Middlesfield Rd., Menlo Park, CA 94025, jachens@usgs.gov
[6] U.S. Geological Survey, 345 Middlesfield Rd., Menlo Park, CA 94025, cwent@usgs.gov

hypocenter. These east-west faults were also recognized by Hardebeck and others (2007) On the basis of seismicity relocated using tomography. On the basis of the existence of these orthogonal conjugate faults, Kilb and Rubin (2002) inferred the growth of a young fault in which slip across the main north-south right-lateral fault is being accommodated on orthogonal east-west-trending cross-faults. Although their existence is contrary to conventional faulting theory, orthogonal conjugate fault pairs do occur in strike-slip systems (Lockwood and Moore, 1979; Nicholson et al., 1986; Thatcher and Hill; 1991). We agree with Kilb and Rubin's (2002) interpretation that the Mt. Lewis fault zone represents a young, vertical right-lateral strike-slip fault zone and present additional geophysical and geologic evidence to support this interpretation.

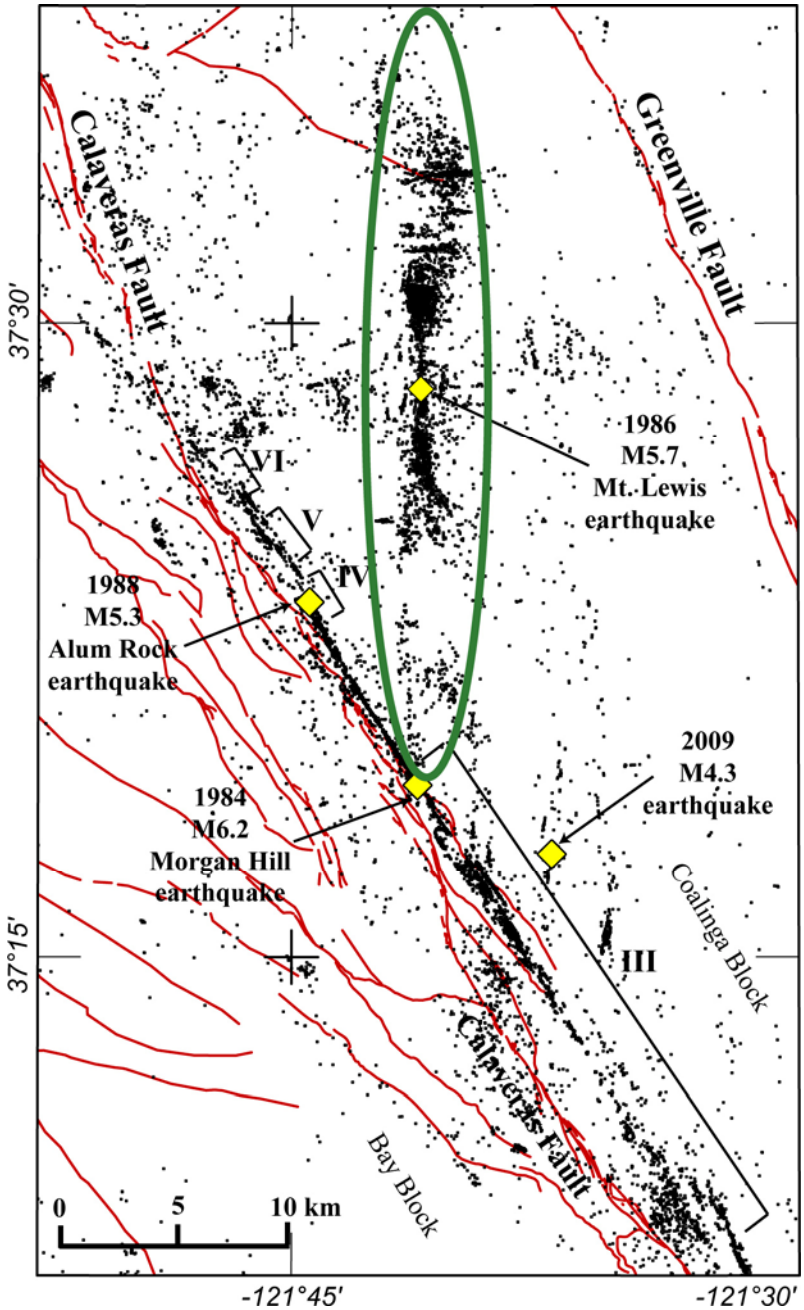

Figure 1. Map of relocated seismicity (black dots, Waldhauser and Schaff, 2008) showing the Mt. Lewis Seismicity Trend (green oval). Roman numerals III-VI represents zones along the Calaveras Fault identified by Oppenheimer et al. (1990). Red lines, Quaternary faults from Graymer et al. (2006).

Based on analysis of the aftershock sequence of the Morgan Hill earthquake, Oppenheimer et al. (1988) inferred a series of north-south-trending faults exhibiting right-lateral focal mechanisms in the upper 5 km northeast of the Calaveras Fault. While Oppenheimer et al. (1988) recognized that the Mt. Lewis earthquake had the same focal mechanism as these north-south faults, they did not go so far as to suggest that the two events might have occurred on the same structure. We present evidence that the northernmost north-south-striking fault identified by Oppenheimer et al. (1988) is in fact the southern continuation of the north-south-striking right-lateral fault zone that ruptured during the 1986 Mt. Lewis earthquake, thus providing additional evidence that strain on the Calaveras Fault is being transferred to the Mt. Lewis fault zone.

METHODS

Fault Mapping

We used relocated seismicity (Waldhauser and Schaff, 2008) recorded between 1984 and 2003 to characterize and map the fault structure of the Mt. Lewis trend, similar to the methods employed by Phelps et al. (2008) to map the Hayward and Calaveras Faults at depth for incorporation into a three-dimensional geologic map. Details of the double-difference earthquake relocation method can be found in Waldhauser and Ellsworth (2000). Kilb and Rubin (2002) only identified these E-W faults north of the 1986 Mt. Lewis hypocenter, therefore, we concentrated our mapping efforts south of the Mt. Lewis epicenter to focus on mapping the north-south structural trends. Fault mapping was carried out in two stages: (1) fault planes were identified on two-dimensional seismicity cross-sections perpendicular to the Mt. Lewis trend, and (2) three-dimensional fault surfaces were constructed based on correlation of fault planes on adjacent cross-sections. Using cross-section slices spaced 1-km apart, oriented perpendicular to the Mt. Lewis trend, we identified alignments in seismicity at depth. Calaveras Fault seismicity was removed from cross-sections within 10 km of the Morgan Hill earthquake prior to interpretation to avoid confusing Mt. Lewis seismicity and Calaveras Fault seismicity. Straight line segments were drawn through those alignments and extended to the surface, representing fault planes. We used 3D viewing software to create three-dimensional fault surfaces by comparing fault planes from adjacent cross sections On the basis of spatial proximity, geometric similarity, and correlation to continuous geologic features mapped at the surface (Wentworth et al., 1999). In places where few or no earthquake hypocenters existed, it was necessary to interpolate among cross-sections.

Magnetic Model

The aeromagnetic data used in this study (Figure 2) are composed of two high-resolution surveys collected by the U.S. Geological Survey (1992, 1996) that have a flight-line spacing of 500 m and a flight-line elevation of 250 m. Aeromagnetic data were reduced to total intensity magnetic field values and include corrections for diurnal variations of the Earth's magnetic field and removal of a regional magnetic field of the Earth using an IGRF 2000 model (Langel, 1992). The magnetic highs (warm colors, Figure 2) represent magnetic basement rocks, such as serpentinite and mafic rocks of the Coast Range Ophiolite and the magnetic lows (cool colors) represent the polarization of magnetic anomalies as well as the relatively non-magnetic alluvial fill and rocks within the Franciscan Complex and Great Valley Sequence.

These magnetic data were used to model the magnetic property distributions associated with subsurface geologic structure, specifically the geometry and depth extent of a serpentinite body along Profile A-A' adjacent to the Mt. Lewis seismicity trend (Figure 2). This model is constrained by surficial geology as mapped by Wentworth et al. (1999). Rock properties were assigned to model blocks based regional and local average densities and magnetic susceptibilities from Carmichael (1982) and Ponce (2004), respectively. In using both geologic and physical property constraints in our modeling, we reduce the ambiguity and non-uniqueness of the resultant model.

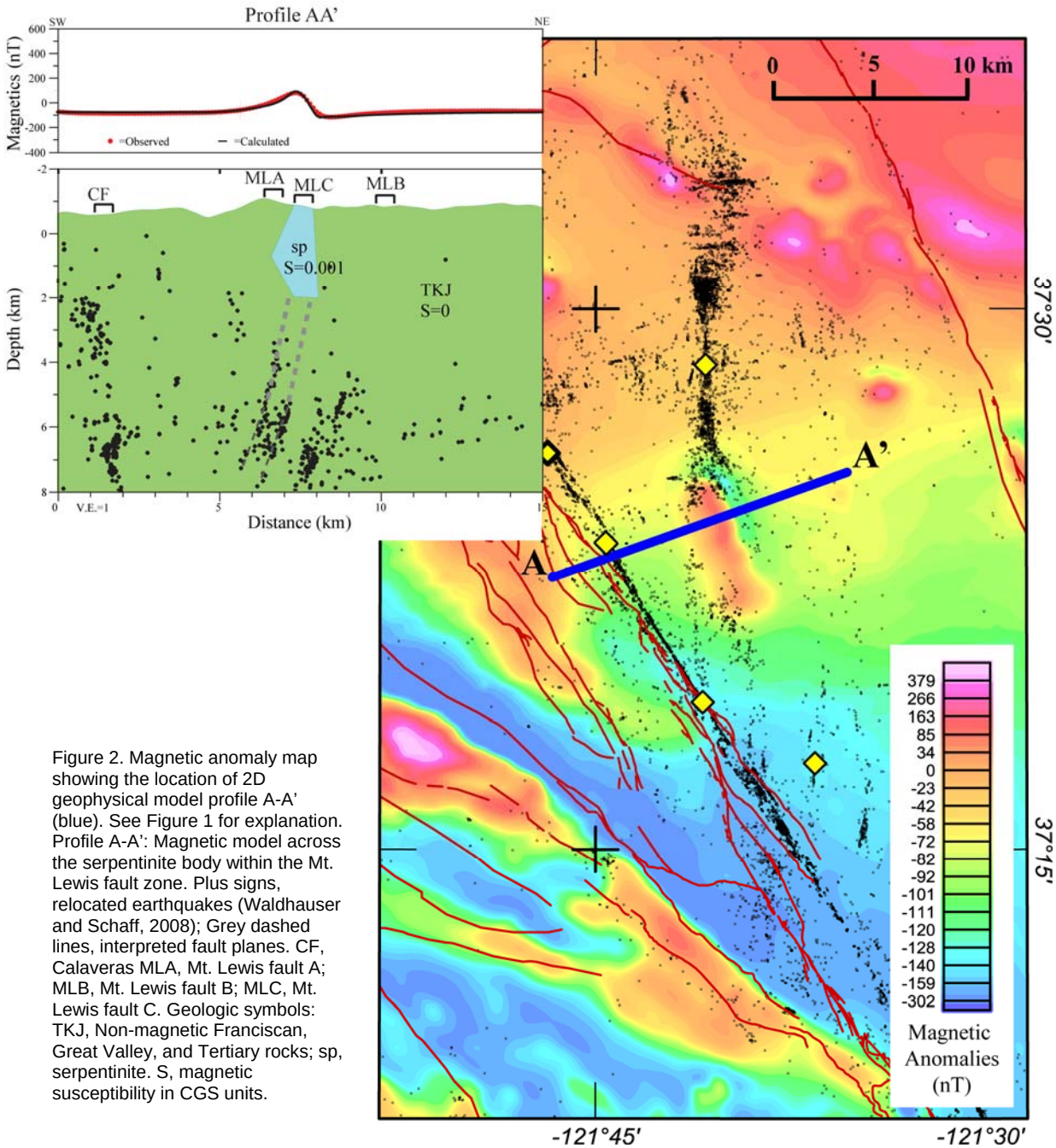

Figure 2. Magnetic anomaly map showing the location of 2D geophysical model profile A-A' (blue). See Figure 1 for explanation. Profile A-A': Magnetic model across the serpentinite body within the Mt. Lewis fault zone. Plus signs, relocated earthquakes (Waldhauser and Schaff, 2008); Grey dashed lines, interpreted fault planes. CF, Calaveras MLA, Mt. Lewis fault A; MLB, Mt. Lewis fault B; MLC, Mt. Lewis fault C. Geologic symbols: TKJ, Non-magnetic Franciscan, Great Valley, and Tertiary rocks; sp, serpentinite. S, magnetic susceptibility in CGS units.

FAULT ZONE CHARACTERIZATION

Using 2D and 3D analysis of double-difference relocated seismicity, we identify three main fault structures extending southward from the epicenter of the 1986 Mt. Lewis earthquake. Alignments of hypocenters reveal a series of steeply dipping fault planes that define a main north-south-trending narrow fault zone, Mt. Lewis fault A (MLA, Figures 3 and 4), consistent with previous interpretations. However, our analysis of seismicity suggests this fault zone extends southward to the Calaveras Fault along the northernmost of a series of north-south-trending faults identified by Oppenheimer et al. (1988) following the 1984 Morgan Hill earthquake. MLA is 25-km long with dips varying from vertical north of the Mt. Lewis epicenter to steeply west-dipping south of the epicenter.

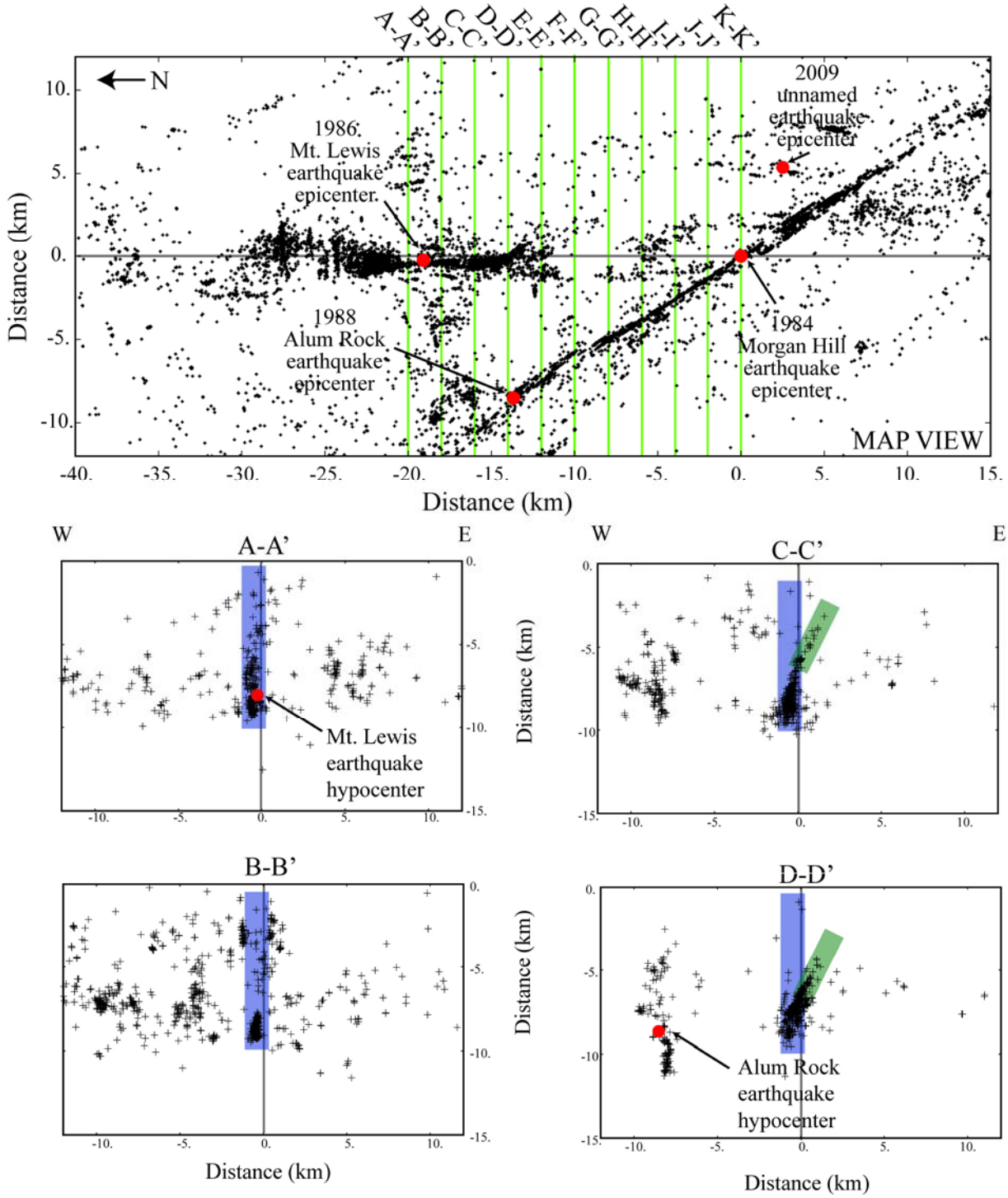
A-A'
B-B'
C-C'
D-D'
E-E'
F-F'
G-G'
H-H'
I-I'
J-J'
K-K'
N
1986
Mt. Lewis
earthquake
epicenter
2009
unnamed
earthquake
epicenter
1988
Alum Rock
earthquake
epicenter
1984
Morgan Hill
earthquake
epicenter
MAP VIEW
Distance (km)
W
E
Mt. Lewis
earthquake
hypocenter
Alum Rock
earthquake
hypocenter

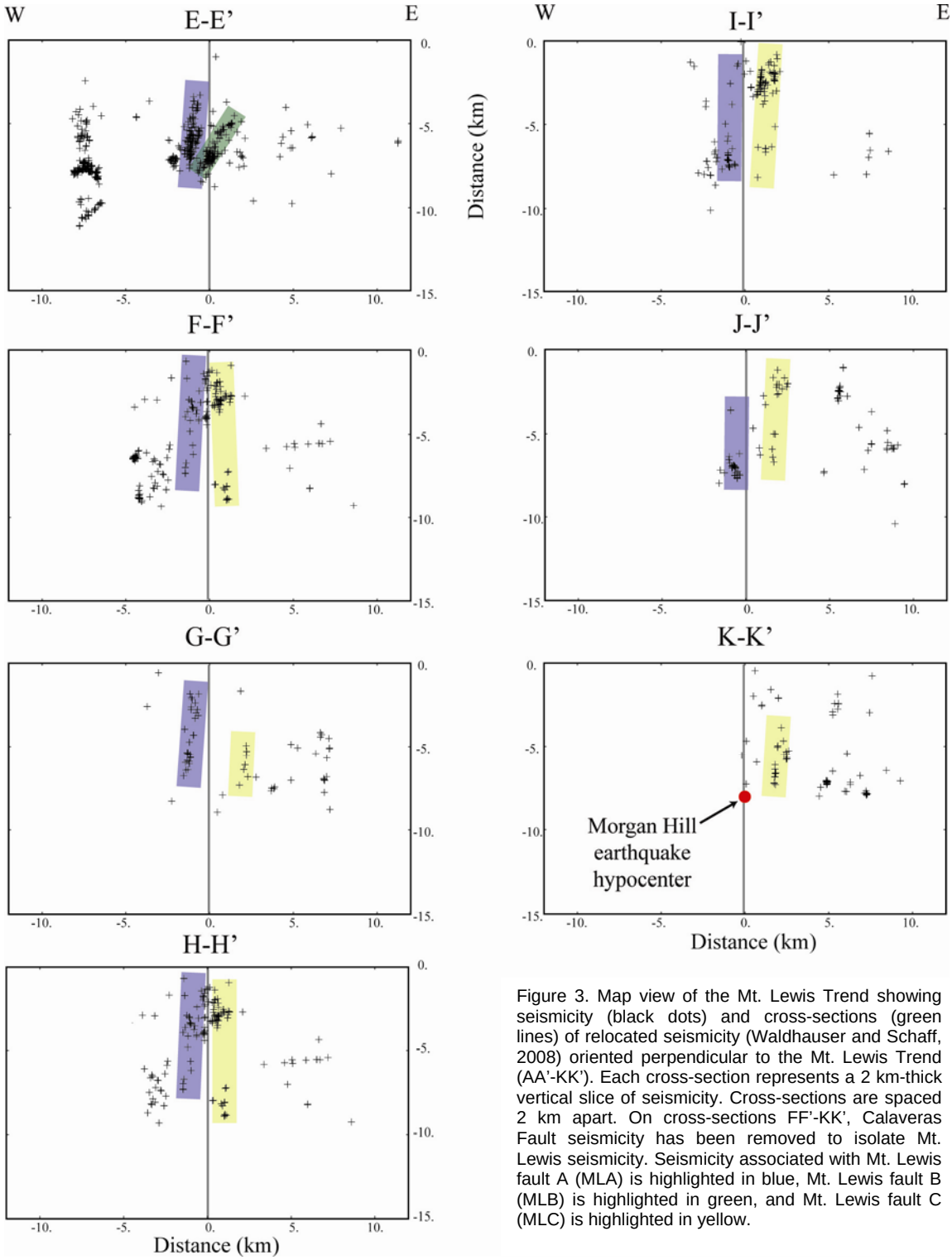

Figure 3. Map view of the Mt. Lewis Trend showing seismicity (black dots) and cross-sections (green lines) of relocated seismicity (Waldhauser and Schaff, 2008) oriented perpendicular to the Mt. Lewis Trend (AA'-KK'). Each cross-section represents a 2 km-thick vertical slice of seismicity. Cross-sections are spaced 2 km apart. On cross-sections FF'-KK', Calaveras Fault seismicity has been removed to isolate Mt. Lewis seismicity. Seismicity associated with Mt. Lewis fault A (MLA) is highlighted in blue, Mt. Lewis fault B (MLB) is highlighted in green, and Mt. Lewis fault C (MLC) is highlighted in yellow.

In addition, seismicity cross sections highlight two additional steeply dipping faults: Mt. Lewis fault B (MLB) and Mt. Lewis fault C (MLC). When these fault planes are extended to the surface, the northern fault, MLB, (Figures 3 and 4) coincides with a north-northwest-trending unnamed fault that was mapped based on the existence of a lineament in Franciscan mélange that exhibits extensive hydrothermal alteration (Wentworth et al., 1999). MLB first appears in cross section just north of profile C-C' and joins MLA at about 6 km depth. This fault is visible on consecutive seismicity cross sections to the south until profile F-F'. MLC can be identified from profile F-F' in the north and extends southward beyond profile K-K', where it appears to join the Calaveras Fault (Figures 3 and 4). Alignments of seismicity along MLC extend to the surface coincident with a locally north-trending lithostratigraphic fault boundary separating serpentinite and distinctive high-grade schist units of the Coast Range Ophiolite from surrounding Franciscan mélange (Wentworth et al., 1999). The

serpentinite/schist unit likely represents a relic subduction fault boundary. Magnetic modeling of the serpentinite indicates a steeply dipping body that extends to at least 2 to 3-km depth, corresponding to alignments of deeper seismicity (Figure 2). On the basis of these findings, deformation along the Mt. Lewis trend may be activating portions of older structures that are suitably aligned in the current stress field.

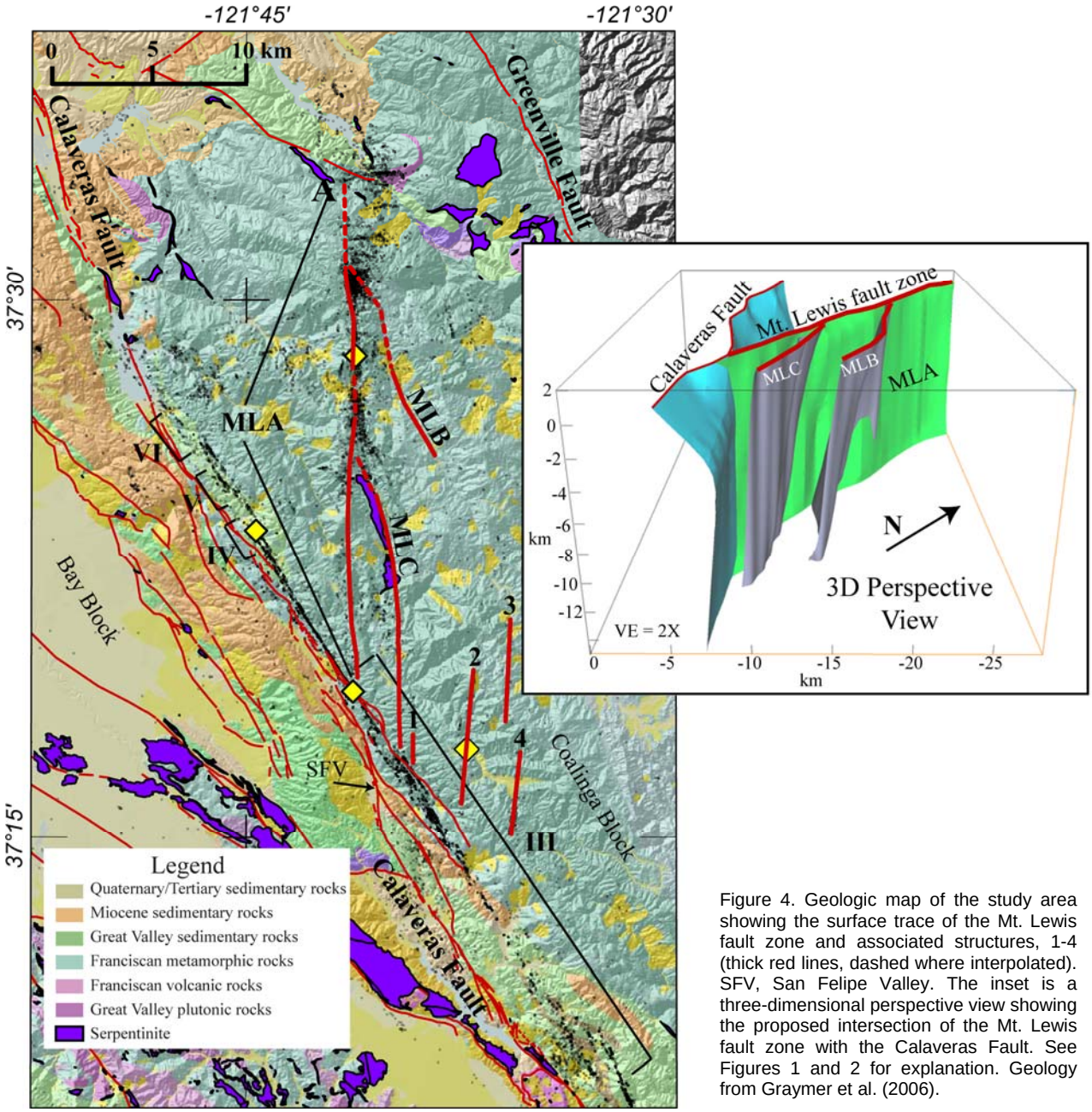

Figure 4. Geologic map of the study area showing the surface trace of the Mt. Lewis fault zone and associated structures, 1-4 (thick red lines, dashed where interpolated). SFV, San Felipe Valley. The inset is a three-dimensional perspective view showing the proposed intersection of the Mt. Lewis fault zone with the Calaveras Fault. See Figures 1 and 2 for explanation. Geology from Graymer et al. (2006).

Although there is no apparent offset in the mapped surface geology or observed surface rupture along the Mt. Lewis trend, a diffuse zone of north-south topographic lineaments that extends the entire length of the Mt. Lewis trend is visible in shaded relief imagery (Figure 5). These lineaments crosscut the structural grain of the surrounding topography, implying a young Mt. Lewis fault zone where just enough offset has occurred to cause differential erosion of the landscape.

The Mt. Lewis seismicity trend is the longest in a series of N-S seismicity trends with right-lateral focal mechanisms located northeast of the Calaveras Fault. On May 30, 2009 there was a M_w 4.3 earthquake south of the Mt. Lewis fault zone on one of these N-S seismicity trends (Figure 1). This event occurred about 3 km east of the Calaveras fault on an unmapped fault defined by a 10 km-long seismicity trend. We identify steeply dipping fault planes associated with four of these north-south seismicity trends, which we refer to as Mt. Lewis-type structures (labeled 1-4 in Figure 4). All of these north-south seismicity trends, including the Mt. Lewis fault zone, occur northeast of the Calaveras Fault along Zone III.

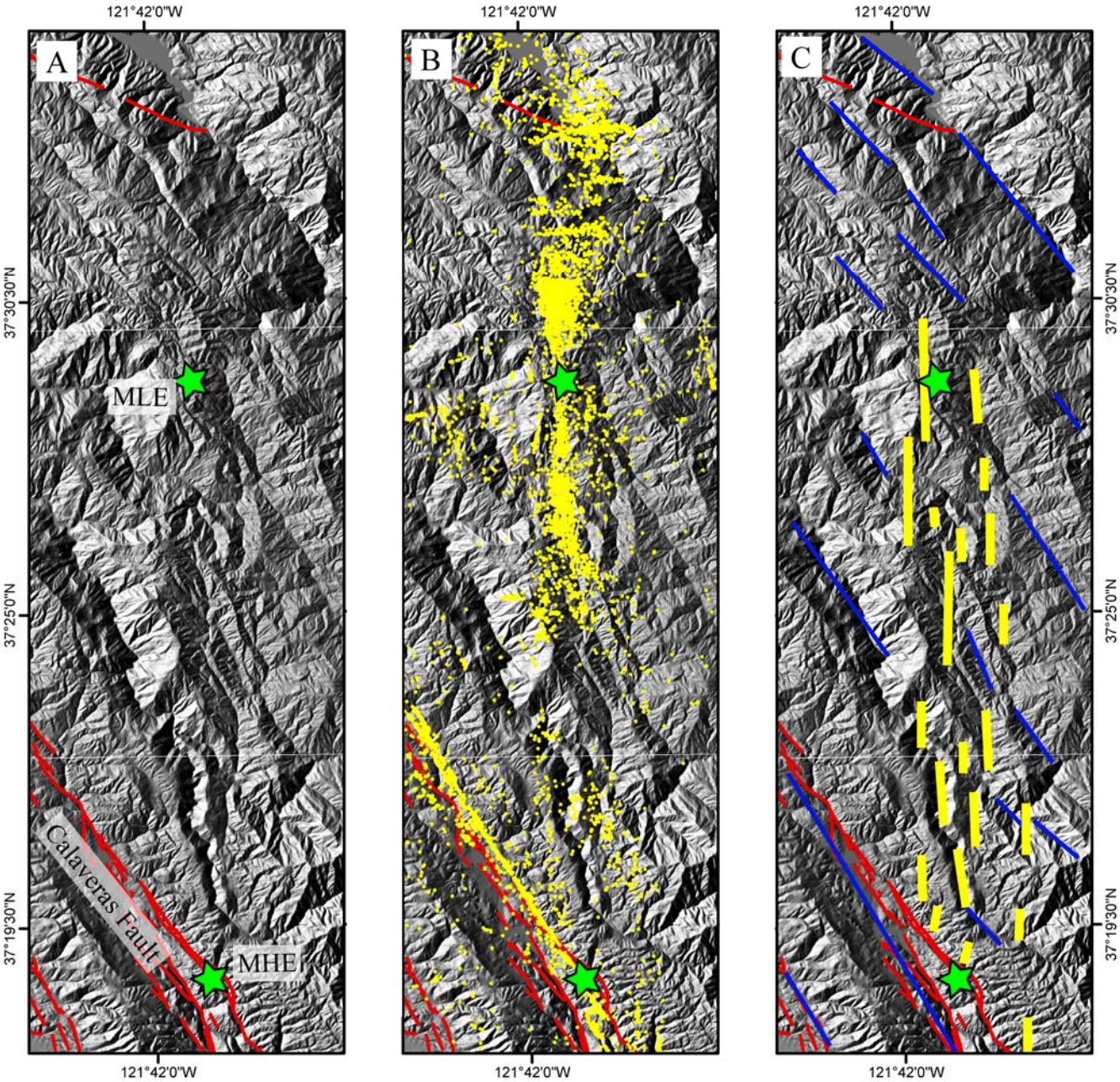

Figure 5. Digital elevation model (DEM) images illustrating the north-south topographic lineaments associated with the Mt. Lewis fault zone. A) DEM image showing Quaternary faults. MLE, 1986 Mt. Lewis earthquake; MHE, 1984 Morgan Hill earthquake. B) DEM image showing relocated seismicity (yellow dots). C) DEM image showing interpreted north-south lineations associated with the Mt. Lewis Trend (thick yellow lines), and lineations representing the more regional northwest-southeast trend (thin blue lines). See figure 1 for explanation.

TECTONIC IMPLICATIONS

On the basis of three-dimensional analysis of earthquake hypocenters, the Mt. Lewis fault zone appears to intersect the Calaveras Fault at a distinctive location, suggesting the two faults are inter-related. The Mt. Lewis fault zone joins the Calaveras Fault near the epicenter of the 1984 Morgan Hill earthquake and at the northern boundary of the Morgan Hill segment (Zone III of Oppenheimer et al., 1990). This conjunction suggests that segmentation on the Calaveras Fault is related to deformation along the Mt. Lewis fault zone. Zone III represents one of six zones (I-VI) along the Calaveras Fault that could produce moderate-sized earthquakes and is defined by the southward-directed rupture of the Morgan Hill earthquake (Oppenheimer et al., 1990). Aftershocks of the Morgan Hill earthquake occurred along the southern Mt. Lewis fault zone and along adjacent north-south-trending faults, providing evidence that slip on Zone III of the Calaveras Fault activates the Mt.

Lewis and related structures. On the basis of Coulomb failure criterion, right-lateral slip on Zone III might have unclamped the Mt. Lewis fault zone, perhaps encouraging the Mt. Lewis earthquake.

Near the Mt. Lewis/Calaveras fault intersection, the surface trace of the Calaveras Fault changes from a northwesterly trend to a more northerly trend across San Felipe Valley (Figures 4 and 5), whereas the seismicity at depth continues uninterrupted on a northwesterly trend. At the southern end of San Felipe Valley, the trace of the Calaveras Fault resumes a northwesterly trend but is offset from the seismicity at depth by about 4 km. This disconnect between the mapped surface trace and seismicity at depth suggests the Calaveras Fault either dips shallowly to the northeast in the upper 1-2 km and then becomes near vertical coincident with the seismicity, or the mapped surface trace represents a distinct western fault plane that is not expressed in the seismicity. Regardless, right-lateral motion on the Mt. Lewis Fault Zone may help explain the westward shift in the surface trace of the Calaveras Fault south of the Morgan Hill epicenter.

Studies using GPS data from the Bay Area velocity unification (BAVU) show that the Coalinga Block on the eastern side of the Calaveras and Mt. Lewis fault zones (Figure 1) is moving southward relative to the Bay block on the western side of the Calaveras Fault (d'Alessio et al., 2005), which is consistent with right-lateral motion on the Mt. Lewis fault zone. The right-lateral motion occurring on the Mt. Lewis fault zone should induce both right-lateral shear and fault-perpendicular compression on Zone III and unclamping on Zone IV to the north (Figures 1 and 4). If there is significant inter-seismic slip along the Mt. Lewis fault zone, as has been suggested for the Calaveras Fault (Manaker et al., 2003), the motions generated by the 1986 Mt. Lewis earthquake could be amplified. Simple dislocation models show that the Morgan Hill earthquake induces right-lateral motion on and unclamping of the Mt. Lewis fault zone and that the Mt. Lewis earthquake unclamps the Calaveras Fault in Zones IV, V, and VI. These observations suggest the 1986 Mt. Lewis earthquake may have unclamped Zone IV and promoted failure in the 1988 M_w 5.3 Alum Rock earthquake.

The apparent interaction between Zone III along the Calaveras Fault and the Mt. Lewis fault zone suggests that strain is being transferred between these two structures. If this is the case, the Mt. Lewis fault zone and other Mt. Lewis-type structures may in turn be transferring strain from the Calaveras Fault to other faults, including the active portion of the Greenville Fault. The emergence of the Mt. Lewis fault zone may help explain why the southern Greenville fault appears to have been abandoned (Graymer et al., 2006). Fault mapping of the Mt. Lewis trend and associated structures has highlighted the development of a complex system of north-south-trending faults and their apparent connection to, and interaction with, Zone III along the Calaveras Fault. If the Mt. Lewis fault zone and related structures are transferring strain between the Calaveras and Greenville faults and are accommodating deformation within the Diablo Range, these structures are likely important and emerging elements in the tectonic framework of the eastern San Francisco bay area. The recent M_w 4.3 event highlights the earthquake potential of these presumably buried north-south faults and the need to integrate these structures into seismic hazard analysis for the San Francisco Bay area.

ACKNOWLEDGMENTS

We would like to thank Jeanne Hardebeck and Darcy McPhee for valuable reviews, which greatly improved this manuscript.

REFERENCES

Carmichael, R.S., 1982, Magnetic properties of minerals and rocks: Boca Raton, Florida, CRC Press.

D'Alessio, M.A., Johanson, I.A., Bürgmann, R., Schmidt, D.A., and Murray, M.H., 2005, Slicing up the San Francisco Bay Area: Block kinematics and fault slip rates from GPS-derived surface velocities: Journal of Geophysical Research, v. 110, 19 p.

Graymer, R.W. Moring, B.C., Saucedo, G.J., Wentworth, C.M., Brabb, E.E., and Knudsen, K.L., 2006, Geologic map of the San Francisco Bay region: U.S. Geological Survey Scientific Investigations Map 2918. [http://pubs.usgs.gov/sim/2006/2918/, last accessed March 9, 2009].

Hardebeck, J.L., Michael, A.J., and Brocher, T.M., 2007, Seismic velocity structure and seismotectonics of the eastern San Francisco Bay region, California: Bulletin of the Seismological Society of America, v. 97, n. 3, p. 826-842, doi: 10.1785/0120060032.

Kilb, D. and Rubin, A.M., 2002, Implications of diverse fault orientations imaged in relocated aftershocks of the Mount Lewis, M_L 5.7, California, earthquake: Journal of Geophysical Research, v. 107, no. B11, p. 17.

Langel, R.A., 1992, International geomagnetic reference field: the sixth generation: Journal of Geomagnetism and Geoelectricity, v.44, no. 9, p. 679-707.

Lockwood, J.P., and J.G. Moore, 1979, Regional deformation of the Sierra Nevada, California, on conjugate microfault sets: Journal of Geophysical Research, v. 84, p. 6041-6049.

Manaker, D. M., Burgmann, R., Prescott, W.H., and Langbein J., 2003, Distribution of interseismic slip rates and the potential for significant earthquakes on the Calaveras fault, central California: Journal of Geophysical Research, v. 108, B6, doi:10.1029/2002JB001749.

Nicholson, C.L., Seeber, Williams, P., and Sykes, L.R., 1986, Seismic evidence for conjugate slip and block rotation within the San Andreas fault system, southern California: Tectonics, v. 5, p. 629-648.

Oppenheimer, D.H., Bakun, W.H., and Lindh, A.G., 1990, Slip partitioning of the Calaveras Fault, California, and prospects for future earthquakes: Journal of Geophysical Research, v. 95, no. B6, p. 8483-8498.

Oppenheimer, D.H. and MacGregor-Scott, Nan, 1992, The seismotectonics of the Eastern San Francisco Bay region, in Borchardt, Glenn, and others, eds: Proceedings of the Second Conference on Earthquake Hazards in the Eastern San Francisco Bay Area: California Department of Conservation, Division of Mines and Geology Special Publication 113, p. 11-16.

Oppenheimer, D.H., Reasenberg, P.A., and Simpson, R.W., 1988, Fault plane solutions for the 1984 Morgan Hill, California, earthquake sequence: Evidence for the state of stress on the Calaveras Fault: Journal of Geophysical Research, v. 93, no. B8, p. 9007-9026.

Phelps, G.A., Graymer, R.W., Jachens, R.C., Ponce, D.A., Simpson, R.W., and Wentworth, C.M., 2008, Three-dimensional geologic map of the Hayward Fault zone, San Francisco Bay region, California: U.S. Geological Survey Scientific Investigations Map 2545. [http://pubs.usgs.gov/sim/2545/, last accessed March 9, 2009].

Ponce, D.A., Simpson, R.W., Graymer, R.W., and Jachens, R.C., 2004, Gravity, magnetic, and high-precision relocated seismicity profiles suggest a connection between the Hayward and Calaveras Faults, Northern California: Geochemistry, Geophysics, Geosystems - G (super 3), v. 5, p. no.7, 39.

Schaff, D.P., Bokelmann, G.H.R., Beroza, G.C., Waldhauser, F., and Ellsworth, W.L., 2002, High-resolution image of Calaveras fault seismicity: Journal of Geophysical Research, v. 107, no. B9, p. 2186, doi:2110.1029/2001JB000633.

Thatcher, W. and Hill, D.P., 1991, Fault orientations in extensional and conjugate strike-slip environments and their implications: Geology, v. 19, p. 1116-1120.

Waldhauser, Felix, and Ellsworth, W.L., 2000, A double-difference earthquake location algorithm: Method and application to the northern Hayward fault: Bulletin of the Seismological Society of America, v. 90, p. 1353-1368.

Waldhauser, F., and Ellsworth, W.L., 2002, Fault structure and mechanics of the Hayward Fault, California, from double-difference earthquake locations: Journal of Geophysical Research, v. 107, no. B3, p. 2054, doi:2010.1029/2000JB000084.

Waldhauser, F., and Schaff, D.P., 2008, Large-scale relocation of two decades of Northern California seismicity using cross-correlation and double-difference methods: Journal of Geophysical Research, v. 113, no. B08311, doi:10.1029/2007JB005479.

Wentworth, C.M, Blake, M.C., Jr., McLaughlin, R.J., and Graymer, R.W., 1999, Preliminary geologic map of the San Jose 30 x 60-minute quadrangle, California; a digital database: U.S. Geological Survey Open-File Report 98-795. [http://pubs.usgs.gov/of/1998/of98-795/, last accessed March 9, 2009].

U.S. Geological Survey and EROS Data Center, 1999, National Elevation Dataset: U.S.Geological Survey. [http://gisdata.usgs.net/ned/ last accessed 6/15/08].

U.S. Geological Survey, 1992, Aeromagnetic map of Livermore and vicinity, California: U.S. Geological Survey Open-File Report 92-531, scale 1:250,000.

U.S. Geological Survey, 1996, Aeromagnetic map of the central San Francisco Bay area, California: U.S. Geological Survey Open File Report 96-530, scale 1:100,000.

Zhou, Y., 1992, Analysis of the 1986 Mt. Lewis, California, earthquake: preshock sequence-mainshock-aftershock sequence: Physics of the Earth and Planetary Interiors, v. 75, p. 267-288.